Human Genomics

RESEARCH Open Access

Sideroflexin family genes were dysregulated and associated with tumor progression in prostate cancers

Hua Huang[1], Huibo Lian[1], Wang Liu[2], Benyi Li[2*], Runzhi Zhu[3] and Haiyan Shao[1*]

Abstract

Sideroflexin (SFXN) family genes encode for a group of mitochondrial proteins involved in cellular processes such as iron homeostasis, amino acid metabolism, and energy production. Recent studies showed that they were aberrantly expressed in certain human cancers. However, there is a paucity of information about their expression in prostate cancer. In this study, we took a comprehensive approach to investigate their expression profiles in benign prostate tissue, prostate-derived cell lines, and prostate cancer tissues using multiple transcriptome datasets. Our results showed that SFXN1/3/4 genes were predominantly expressed in prostate tissue and cell lines. SFXN2/4 genes were significantly upregulated while the SFXN3 expression was significantly downregulated in malignant tissues compared to benign tissues. SFXN4 expression was identified as a diagnostic biomarker and prognostic factor for unfavorite survival outcomes. In advanced prostate cancers, SFXN2/4 expressions were positively correlated with the androgen receptor signaling activity but negatively correlated with the neuroendocrinal features. Further analysis discovered that SFXN5 expression was significantly elevated in neuroendocrinal prostate cancers. In conclusion, SFXN2/4 expressions are novel biomarkers in prostate cancer diagnosis and prognosis.

Keywords Prostate cancer, Sideroflexin family genes, Castration-resistance, Neuroendocrinal progression, Androgen receptor modulation

Introduction

The sideroflexin (SFXN) family is a group of proteins that are found in the mitochondria of eukaryotes and are involved in cellular processes such as iron homeostasis, amino acid metabolism, and energy production [1]. SFXN proteins are multi-spanning transmembrane proteins with the N-terminus inside the cytoplasm and the C-terminus outside the cytoplasm [1].

SFXN proteins are highly conserved across eukaryotes and include five proteins in humans: SFXN1, SFXN2, SFXN3, SFXN4, and SFXN5 [2]. SFXN1, SFXN2, and SFXN3 are mitochondrial serine transporters that are important for one-carbon metabolism [1, 2]. Studies suggest that their role as a serine transporter and interaction with mitochondrial proteins could make it a target for treatments that address mitochondrial dysfunction common in neurodegenerative conditions [3].

SFXN4 is a complex I assembly factor that helps incorporate the ND6 subunit into complex I [4, 5]. The study of SFXN proteins is an emerging research field that could lead to discoveries about mitochondrial

*Correspondence:
Benyi Li
bli@kumc.edu
Haiyan Shao
Shaoh838@126.com
[1] Urology & Nephrology Center, Department of Urology, Zhejiang Provincial People's Hospital, The Affiliated People's Hospital, Hangzhou Medical College, Hangzhou 310014, Zhejiang, China
[2] Department of Urology, The University of Kansas Medical Center, Kansas City, KS 66160, USA
[3] The Children's Hospital, Zhejiang University School of Medicine, Hangzhou 310052, Zhejiang, China

physiopathology [1, 5]. Mutations in SFXN4 can cause mitochondrial disease, including impaired mitochondrial respiration and hematopoietic abnormalities [1, 4]. SFXN4 deficiencies impact erythroid differentiation, as shown in studies on anemia and mitochondriopathies where SFXN4 disruption affects iron-sulfur (Fe–S) cluster biogenesis [4]. This links SFXN4 to broader metabolic and redox processes across various conditions, underscoring its therapeutic potential in diseases beyond cancer [6].

SFXN5, identified as a citrate transporter in vitro, is critical for neutrophil spreading, an initial step in adhesion and migration essential for immune response. In a recent study, SFXN5 deficiency in neutrophils (induced via siRNA or morpholino injection in mice and zebrafish models) led to impaired cell spreading, adhesion, chemotaxis, and reactive oxygen species (ROS) production [7]. This deficiency also reduced actin polymerization due to lower cytosolic citrate levels and downstream metabolites like acetyl-CoA and cholesterol, which are necessary for actin polymerization mediated by phosphatidylinositol 4,5-bisphosphate (PI(4,5)P2). Supplementing with citrate or cholesterol partially restored these processes, highlighting SFXN5's pivotal role in cellular actin dynamics and neutrophil migration during inflammatory responses.

Identifying novel prognostic biomarkers for prostate cancer is a dynamic and rapidly evolving field. Advances in genomics, proteomics, metabolomics, and imaging, combined with computational innovations, are driving the discovery of more accurate and reliable biomarkers [8, 9]. These novel markers hold the promise of improving prognostic accuracy, guiding personalized treatment, and ultimately enhancing survival and quality of life for prostate cancer patients [10]. Continued research, validation, and integration into clinical practice are essential to realize the full potential of these emerging biomarkers [11].

Currently, there is a paucity of information in the literature about the expression profiles and clinical significance of SFXN family genes in prostate cancers. In this study, we took a comprehensive approach of utilizing multiple transcriptome datasets and analyzed the expression profiles of SFXN family genes in prostate cancers, ranging from benign prostate tissue, and primary cancer to advanced castration-resistant stage. Our results revealed that SFXN2/SFXN4 genes were highly upregulated in prostate cancers. Their expressions were androgen responsive under the modulation of the androgen receptor (AR) signal pathway. High levels of their expression were associated with disease progression to the CRPC stage and worse overall survival outcomes in primary cancers.

Materials and methods

Gene expression profiles in prostate tissue, cancer cell lines, and prostate cancer tissues

Cell-specific analysis of gene expression was conducted using the NCBI GEO dataset #GDS1973 [12]. Four basic cell types were separated with magnetic cell sorting (MACS) based on cell-type specific cluster designation (CD) antigens, integrin beta4 for basal cells, dipeptidyl peptidase IV for luminal secretory cells, integrin alpha-1 for stromal fibromuscular cells, and PECAM-1 for endothelial cells, as described [12]. Gene expression of MACS-sorted cell populations was assessed with Affymetrix Human Genome U133 Plus 2.0 Array (HG-U133Plus2). The microarray data were downloaded from the NCBI GEO site, and the relative values of gene expression were calculated against the control group.

Gene expression of prostate cell lines was analyzed using the Cancer Cell Line Encyclopedia transcriptome dataset [13]. The RNA-seq RPKM values (reads per kilobase per million mapped reads) of gene expression were downloaded on the cBioportal platform (www.cbioportal.org/). There was one benign prostate epithelial cell line (PRECLH) and seven prostate cancer cell lines.

We used the Cancer Genome Atlas program (TCGA-PRAD) RNA-seq dataset to examine the expression profiles of the SFXN family genes in primary prostate cancer, as described in our recent publications [14–22]. Gene expression levels were compared using two approaches, case-matched pair comparison (52 cases) and group cohort comparison (500 patient cases) with 52 benign samples. Statistical analysis and data visualization were conducted on the XIANTAO online platform (https://www.xiantaozi.com/). A comparison of gene expression levels in subgroups stratified by molecular signatures (distinct gene fusion and common mutations) was conducted on the UALCAN platform (https://ualcan.path.uab.edu/).

Patient survival outcome assessment

We examined the association of gene expression with patient survival outcomes, including overall survival, disease-specific survival, and progression-free interval. Patients were stratified using the minimum *p*-value cutoff approach [23]. The Kaplan–Meier curve analysis and ROC-based prediction were performed on the XIANTAO platform. The results were visualized with the survminer package and ggplot2 package of the R package (version 4.2.1).

Gene expression analysis in CRPC and NEPC tissues

We used the SU2C/PCF RNA-seq dataset [24] for the analysis of SFXN gene expression at the mRNA levels in CRPC patients on the cBioportal platform. Patients were

divided into different subgroups based on pathological subtype, androgen receptor (AR) signaling activity score, and neuroendocrinal feature of prostate cancer (NEPC) score for comparison. Correlation analysis between gene expression levels and AR score or NEPC score was conducted in categories of Spearman and Pearson coefficients on the cBioportal platform.

Gene expression profiling in single-cell sequencing datasets was conducted using the Human Prostate Single cell Atlas (HuPSA) online database (https://pcatools.shinyapps.io/HuPSA-MoPSA/), as described in a recent report [25]. This online database also contains a bulk RNAseq dataset derived from 877 human prostatic specimens (ProAtlas).

Gene expression in mouse prostate tissue and human prostate cancer xenografts after castration

Gene expression analysis in mouse prostate tissues was conducted using the NCBI GEO dataset GDS#2562, as described previously [26]. Briefly, C57/B6 mice were sham-operated or castrated, and mouse prostate tissues were harvested at 3 or 14 days after surgery. One group of animals was implanted with testosterone (T) pellet at 15 mg/pellet/mouse at day 14 post-surgery for three days before tissue harvesting. Total RNA was purified with the RNeasy kit (Qiagen, Valencia, CA) for the Affymetrix MGU74A chip-based gene analysis.

LuCaP35 xenografts were established in NOD/SCID mice [27]. After sham operation or castration, xenograft tumors were harvested for RNA extraction using the QIAGEN RNeasy Mini Kit (Valencia, CA), followed by GeneChip assays using the Affymetrix human genome U133 Plus 2.0 array. The results were downloaded from the NCBI GEO profile GDS#4120.

KUCaP-2 xenograft models with wild-type AR were established subcutaneously in nude mice [28]. Animals bearing KUCaP-2 xenograft tumors were castrated and xenograft tumor tissues were harvested at 3–5 months post-surgery. Total RNA was isolated and purified using the RNeasy Mini Kit (Qiagen) for cDNA microarray analysis with an Affymetrix Human Genome U133 Plus2.0, as described [28]. The data were downloaded from the NCBI GEO profile GDS#4107.

DepMap data analysis for gene knockout effect on cellular survival

We utilized the gene effect scores derived from CRISPR knockout screens published by Broad's Achilles and Sanger's SCORE projects [29, 30]. Scores are normalized such that nonessential genes have a median score of 0 and independently identified common essential genes have a median score of -1. Gene effect scores were inferenced by Chronos [30]. Integration of the Broad and Sanger datasets was performed, as described [29]. Negative scores imply cell growth inhibition and/or death following gene knockout. The gene effect data were downloaded from the UALCAN platform.

Real-time quantitative PCR analysis

Human benign prostate epithelial cell line BPH1 and prostate cancer cell lines, LNCaP, 22RV1, C4-2B, PC-3, DU145, and NCI-H660 were purchased from the ATCC (Manassas, VA) and maintained as described in our previous publications [31, 32]. Exponentially grown cells were harvested for total cellular RNA extraction using the TRIZOL protocol as described [33]. Real-time quantitative PCR experiments were conducted using the System QuantStudio5 DX Real-Time PCR system (AppliedBiosystems, Waltham, MA) with the primer pairs shown in Table 1.

Statistical analysis

Gene expression at the mRNA levels was used as $\log_2$ [TPM + 1]) value and presented as the MEAN ± the SEM (standard error of the mean). ANOVA analyses were conducted for multiple group comparisons. Student *t*-test was performed to determine the significance of the differences between the two groups. For data without normal distribution, the Wilcoxon rank sum test was utilized for the statistical analysis. The results were visualized using the ggplot2[3.3.6], stats [4.2.1], and car [3.1–0] from the R package (version 4.2.1). GraphPad software (version 9.1.0) was used for the graphic presentation.

Results

SFXN1/SFXN3/SFXN4 genes are highly expressed in benign prostate tissues and cancer cell lines

To obtain the expression profiles of SFXN family genes in human prostate tissue, we first analyzed the single-cell RNA-seq data derived from NCBI GEO dataset GDS1973 [12]. Prostatic basal, luminal secretory, stromal fibromuscular, and endothelial cell types were separated with magnetic cell sorting (MACS) approach based on cell-type specific cluster designation (CD) antigens. The analysis results showed that SFXN1 and SFXN4 genes were predominantly expressed in prostate tissues followed by SFXN3, while SFXN2 and SFXN5 were expressed at a very low level (Fig. 1A). The secretory luminal cells mainly expressed SFXN1/SFXN4 genes (Fig. 1B), but basal cells expressed only moderate levels of SFXN4/SFXN1 genes (Fig. 1C). However, the SFXN3 gene was relatively enriched in basal cells. The endocrinal cells expressed higher levels of SFXN1 than other cell types.

In human prostate epithelial and cancer cell lines, SFXN1/SFXN4/SFXN5 genes were expressed at higher

Table 1 The primer sets for quantitative PCR

	Sequence (5′—> 3′)	Length	Tm	Location
SFXN1 Primer Pair				
PrimerBank ID196259B18c3				
Amplicon Size 76				
Forward Primer	TTCAATG CCGTCGTCAATT ACA	22	60.6	379–400
Reverse Primer	CGTAAG CTGTTCCCAACT CAT	21	60.0	454–434
SFXN2 Primer Pair				
PrimerBank ID 197927250c3				
Amplicon Size 126				
Forward Primer	CCATAG G CATCACCCAAGT AGT	22	61.2	665–686
Reverse Primer	CGTG CAG G ACCTTG ACT TTC	20	60.9	790–771
SFXN3 Primer Pair				
PrimerBank ID49472836c2				
Amplicon Size 93				
Forward Primer	ATCGTGCAGAACTACAGGGC	20	61.9	157–176
Reverse Primer	ATG G AAG G CG G AGTCAT ACAC	21	61.6	249–229
SFXN4 Primer Pair				
PrimerBank ID47458810c2				
Amplicon Size 14D				
Forward Primer	ACG CCACTG AAAG G G ATCAAG	21	62.4	376–396
Reverse Primer	ACGGCTCCCG CCATTAGTA	19	62.8	515–497
SFXN5 Primer Pair				
PrimerBank ID 93277092c1				
Amplicon Size 88				
Forward Primer	ATG G CG G ATACAG CG ACTAC	20	61.5	1–20
Reverse Primer	GTTTGCCCAGTTGGAAAG GAG	21	61.4	88–68

levels than SFXN2/SFXN3 genes, of which SFXN3 gene was expressed at a very low level (Fig. 1D), indicating a less functional significance. In CRISPR/Cas9-based knockout screening experiments, the SFXN2 gene was identified as a survival-essential gene in all tested prostate benign and malignant cell lines (Fig. 1E), indicating that the SFXN2 gene is critical for cellular survival [34, 35] while the functionalities of SFXN1/SFXN3/SFXN4/SFXN5 genes might be compensated by other isoforms.

SFXN2/SFXN3/SFXN4 genes were aberrantly expressed in primary prostate cancers

We then examined the expression profiles of SFXN family genes in primary prostate cancers using the TCGA-PRAD RNA-seq dataset. We first compared their expression levels in 52 case-matched pairs of benign and malignant tissues from patients who received radical prostatectomy. Our analysis revealed that SFXN2 and SFXN4 genes were significantly upregulated in malignant tissues (Fig. 2A), especially the SFXN4 gene whose upregulation was constantly seen in all cases. In contrast, the SFXN3 gene was sharply downregulated in malignant tissues. We then conducted a group cohort comparison of 502 malignant tissues with benign tissues. The results showed a similar trend of dysregulation of these three genes in prostate cancers (Fig. 2B). SFXN1 and SFXN5 genes did not show a significant alteration. ROC analysis indicated that SFXN4 gene expression had the highest AUC value of 0.877 in distinguishing malignant from benign tissues (Fig. 2C), representing a potential diagnostic biomarker.

We also analyzed the alterations of these genes in distinct molecular subtypes of prostate cancer stratified by unique genetic abnormalities [36]. Although SFXN1 expression did not show a significant alteration in group cohort comparison (Fig. 2B), it was significantly upregulated in the subtypes of ERG, ETV1, and FLI1 fusion-positive cancers (Fig. 3A). Upregulations of SFXN2 and SFXN4 genes were observed in all subtypes except the IDH1 mutant subtype while SFXN3 downregulation was not observed in the subtypes of FLI fusion and IDH1 mutants (Fig. 3B–D). SFXN5 upregulation was observed only in the ERG fusion-positive subtype (Fig. 3E). The mechanisms for the potential regulation of ERG fusion on SFXN5 expression as well as IDH1 mutation on SFXN2/SFXN4 expression are worthy of further investigation.

We finally compared the expression levels of altered SFXN2/3/4 genes in different Gleason score groups. All subgroups with different Gleason scores consistently showed SFXN2/4 upregulation and SFXN3 downregulation (Fig. 3F–H), of which SFXN4 expression showed a gradually increasing trend along with Gleason scores (Fig. 3H). These data suggest that SFXN4 expression is tightly correlated with disease progression.

SFXN1/SFXN3/SFXN4 expressions were correlated with immune infiltration in prostate cancers

We analyzed the correlations of SFXN gene expression with tumor immune infiltrations. The results showed that SFXN1 and SFXN2 shared very similar correlations with the top four (Tcm/T-helper/Th2/Eosinophil) and bottom four (Cytotoxic/NK CD56bright/NK/pDC) immune infiltrations (Fig. 4A, B), however, SFXN1 showed a very strong correlation with top two infiltrations (Spearman $r = 0.445/0.589$, Fig. 4A). SFXN3 expression exerted a very broad and strong (coefficient $r > 0.3$) correlation with more than half of immune infiltrations that were proinflammatory lymphocytes (Fig. 4C). In contrast, SFXN4 expression was negatively correlated with all but two immune infiltrations (Th2/Th17), of which three

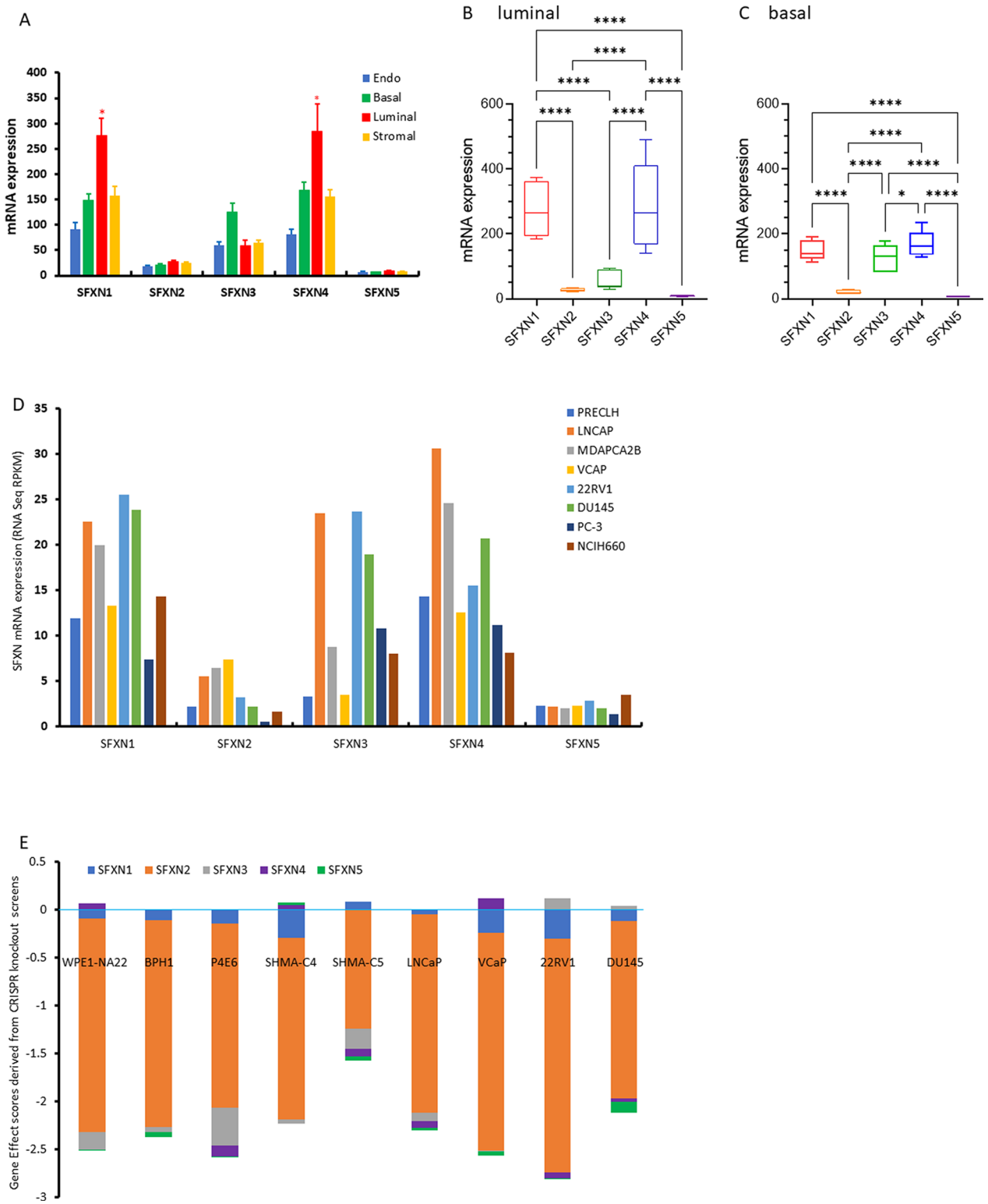

Fig. 1 Expression of SFXN family genes in benign prostate tissue and prostate cancer cell lines. **A**–**C** The expression levels of SFXN family genes were downloaded from the cBioportal platform and RNA-seq RPKM values were utilized for the analysis. ANOVA test, * $p < 0.05$; **** $p < 0.0001$. **D** Real-time qPCR experiments were conducted using the cellular RNAs extracted from prostate cell lines as indicated. **E** DepMap data gene knockout effect was downloaded from the UALCAN platform

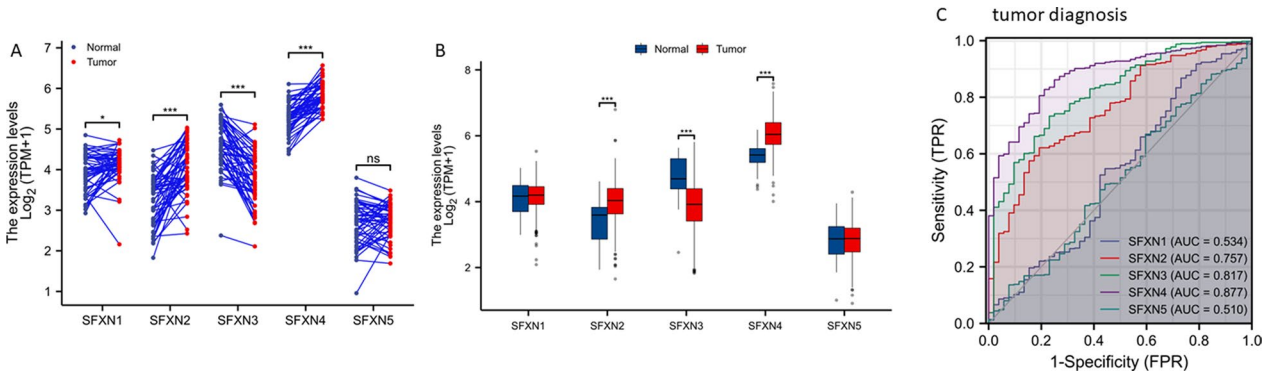

Fig. 2 Expression of SFXN family genes in primary prostate cancers. Case-matched pairs (**A**) or group cohort (**B**) comparisons were conducted between benign and malignant tissues using the TCGA-PRAD dataset (log_2 [TPM + 1]). The asterisks indicate a significant difference compared to the control group. * $p < 0.05$; ***, $p < 0.001$. **C** ROC analysis was conducted to determine the potential of prediction in distinguishing benign and malignant prostate tissues

pro-inflammatory immune infiltrations showed a strong reverse correlation (Spearman r > −0.3, Fig. 4D). SFXN5 expression only exhibited very mild correlations with immune infiltrations (Fig. 4E). These data suggest that SFXN1 and SFXN2 shared a very similar correlation with immune infiltrations while SFXN3 was positively associated but SFXN4 was negatively associated with pro-inflammatory lymphocytes.

To understand if SFXN family genes were expressed in these immune infiltrated cells, we analyzed the signal cell sequence dataset derived from prostate cancer tissues [25], available on the Human Prostate Single-cell Atlas (HuPSA) platform. As shown in Fig. 4F, SFXN1 expression was mainly found in the proliferating T lymphocytes, and other SFXN family members were only slightly expressed in immune infiltrated lymphocytes (Fig. 4G–J). These data suggest that SFXN family genes were not highly expressed in immune infiltrations other than SFXN1 in proliferating T cells.

SFXN4 expression was a worse prognostic factor in prostate cancer

We conducted the Kaplan–Meier survival curve-based prognosis analysis with the TCGA-PRAD dataset. Our results showed that higher levels of SFXN4 expression were associated with worse overall survival outcomes in prostate cancer patients (Fig. 5A). In addition, a borderline significance ($p = 0.051$) was observed in progression-free interval outcomes (Fig. 5B). ROC prediction model analysis indicated that SFXN4 expression had the best AUC value (0.770) as a predictor for a 10-year disease-specific survival prognosis. These data suggest that SFNX4 might serve as a moderate prognostic factor for prostate cancer outcome.

SFXN2/4 expression was associated with CRPC progression

Castration-resistant progression followed by neuroendocrinal (NE) trans-differentiation is the major clinical obstacle in prostate cancer management [37, 38]. We analyzed the expression levels of SFXN family genes in CRPC tissues using the SU2C/PCF RNA-seq dataset [24]. Our analysis found that SFXN2/SFXN4 expressions were positively while SFXN3 expression was negatively correlated with AR signaling scores with a very strong co-efficient (Fig. 6A–C). In addition, a strong and negative correlation was observed between SFXN2/SFXN4 expressions and NEPC scores (Fig. 6D, E). These data indicated that SFXN2/SFXN4 expressions were strongly associated with prostate cancer progression.

We then examined the associations of SFXN family gene expressions with NE features. Our results showed that SFXN1/SFXN5 expression levels were higher but SFXN4 expression was lower in NE feature-positive cancers than those without NE features (Fig. 7A–E). Consistently, the results from another RNA-seq dataset (ProAtlas) also showed these alterations of SFXN family gene expression in NEPC tissues (Fig. 7F–J). Specifically, SFXN1 expression was significantly elevated in NEPC tissues (Fig. 7F), including two newly identified double-negative KRT7 and Progenitor-like subtypes [25]. Interestingly, SFXN2 expression was increased in Progenitor-like NEPCs compared to CRPC tissues while its expression was gradually decreased in CRPC along with the increasing Gleason scores (Fig. 7G), which is in line with the whole genome RNAseq data (Fig. 3F). SFXN3 downregulation and SFXN4 upregulation in CRPC tissues were also observed (Fig. 7H, I), which is in line with the whole genome RNA-seq analysis (Fig. 3G, H). SFXN5 expression was significantly higher in NEPC tissues plus the KRT7 subtype (Fig. 7J), which is also in line with the

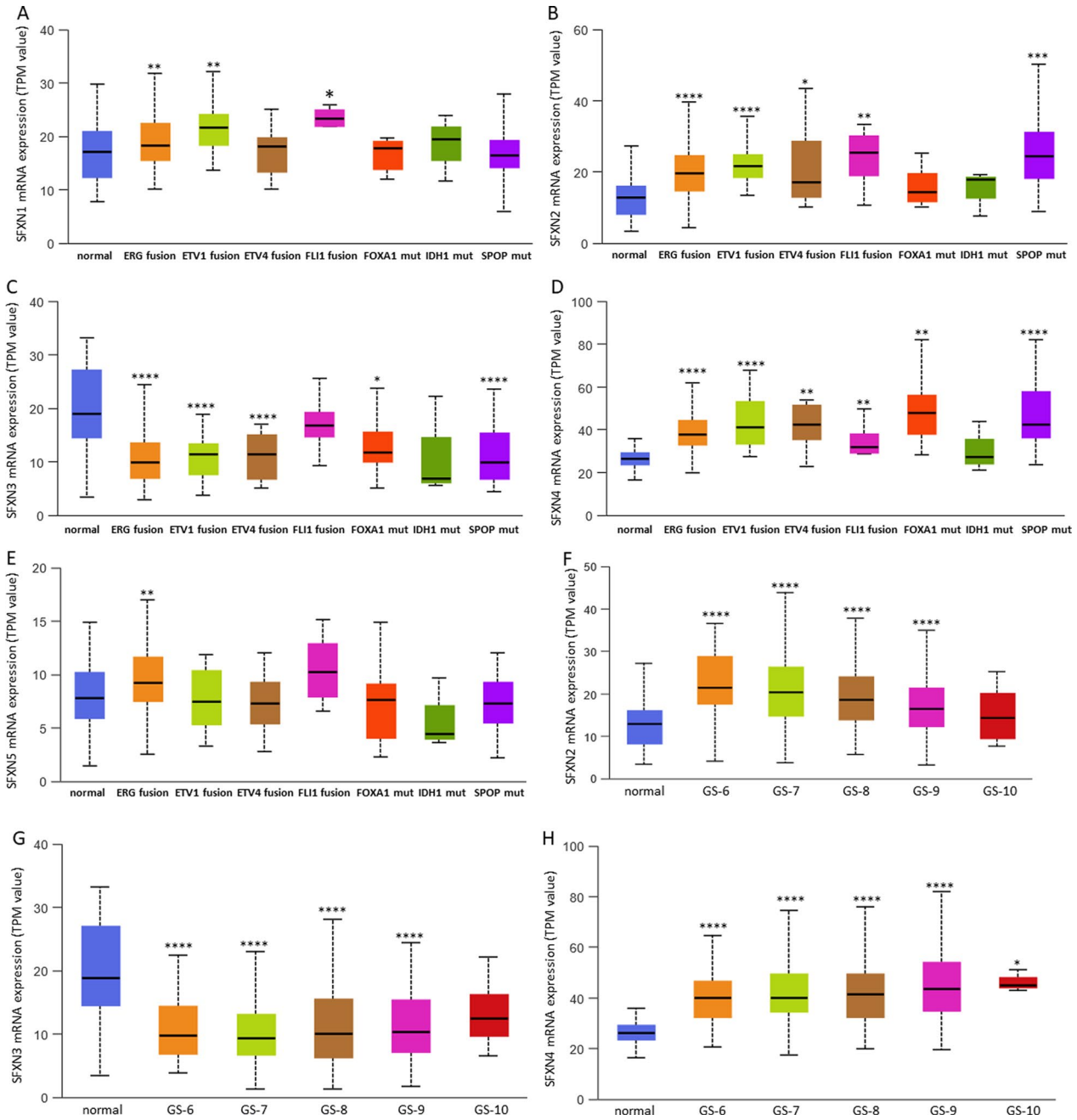

Fig. 3 Expression of SFXN family genes in subgroups with specific molecular signatures or different Gleason scores. **A**–**E** SFXN expresion in different molecular signature groups. **F**–**G** SFXN2/3/4 expression in different Gleason score groups. Gene expression data was downloaded from the TCGA-PRAD dataset on the UALCAN platform. The asterisks indicate a significant difference compared to the benign group. * $p < 0.05$; ** $p < 0.01$; ***, $p < 0.001$; ****$p < 0.0001$. The case numbers in each group: normal (52), ERG (152), ETV1 (28), ETV4 (14), FLI (4), FOXA1 (9), IDH1 (3), and SPOP (35)

data showing higher SFXN5 in NEPC cell line NCI-H660 (Fig. 1D).

Finally, we examined the castration effect on SFXN family gene expression. A microarray dataset derived from mice prostate tissues [26] was utilized to analyze SFXN family gene expression. As shown in Fig. 8A, castration of the animals significantly reduced SFXN2 expression at 3–14 days after surgery and testosterone replacement for 3 days largely restored SFXN2 expression. These data suggest that the SFXN2 gene

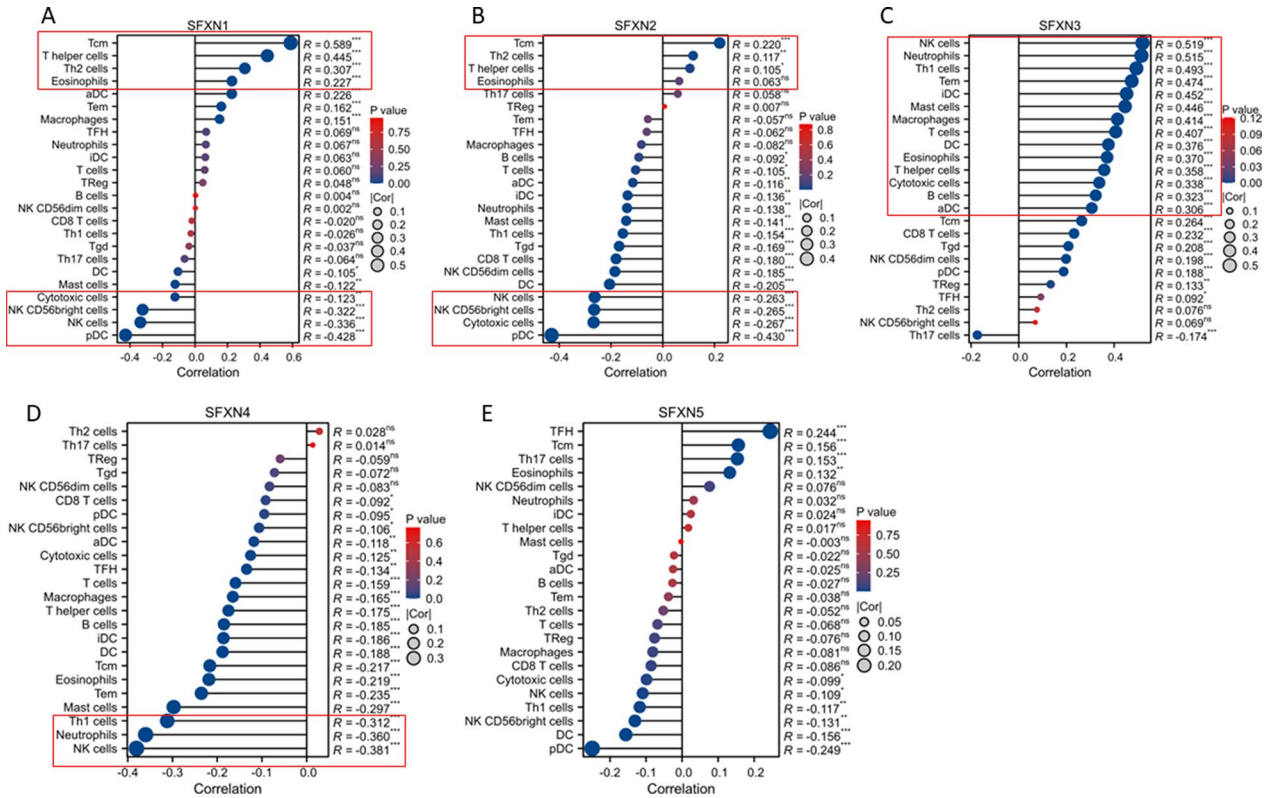

Fig. 4 Correlations of SFXN family genes with tumor immune infiltrations in prostate cancers. **A**–**E** The TCGA-PRAD RNS-seq dataset was utilized for the correlation analysis with tumor immune infiltrations on the XIANTAO platform. The red line squares indicated special factors with SFXN gene expression. **F**–**J** Single-cell sequencing data of gene expression in the immune infiltrations were downloaded and visualized using the online HuPSA database

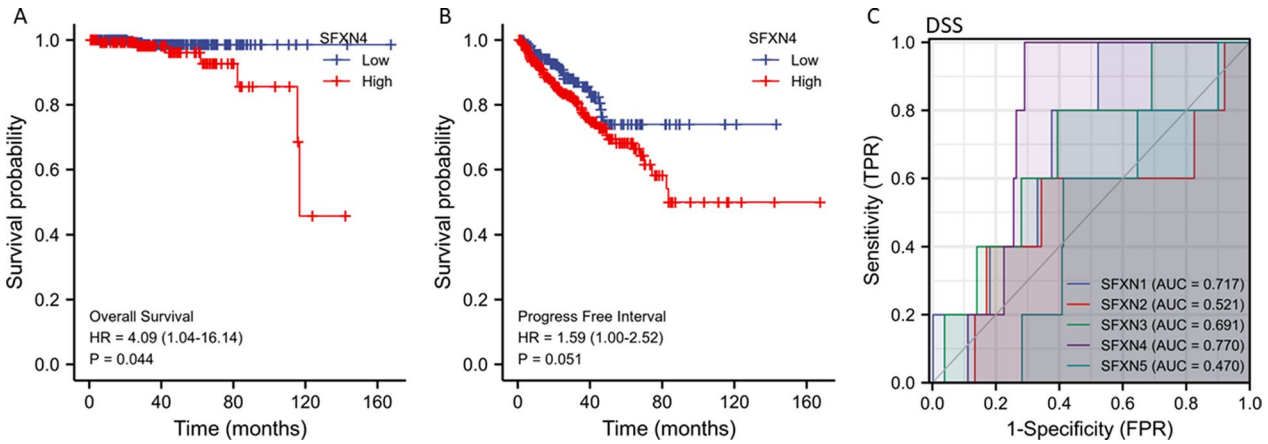

Fig. 5 Kaplan–Meier survival analysis. SFXN4 expression as prognostic factor for overall survival (**A**), diseasespecific survival (**B**) and progression-free interval outcomes (**C**). Gene expression data for the SFXN4 expression were extracted from the TCGA-PRAD RNA-seq dataset. Kaplan-Meier survival curves were generated with a minimum *p*-value approach on the XIANTAO platform

was modulated by androgens. In addition, we analyzed SFXN4 expression in two different human prostate cancer xenograft models, KUCaP-2 [28] and LuCaP35 after castration [27]. The results showed that castration of the animals significantly reduced SFXN4 gene expression in the xenograft tissues (Fig. 8B, C). These data suggest that SFXN2 and SFXN4 expressions were modulated by the androgens.

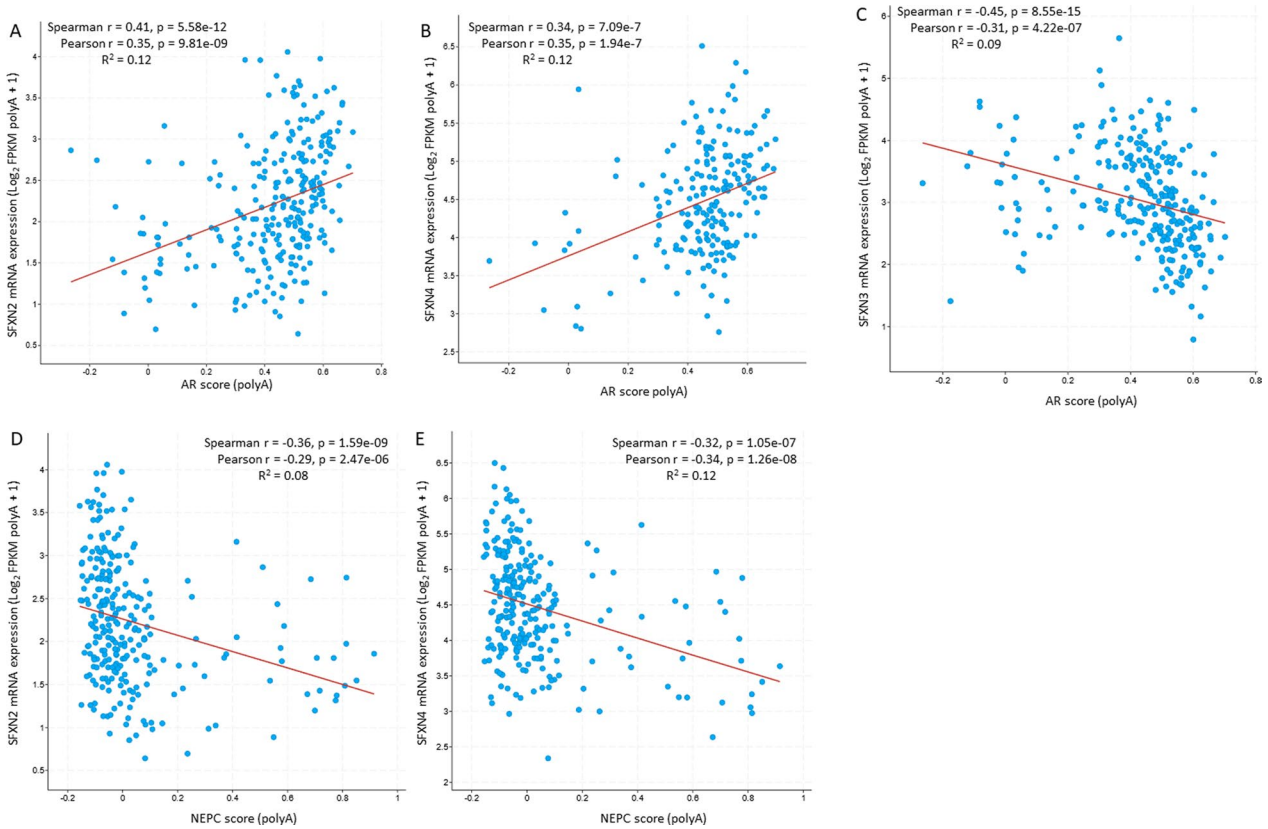

Fig. 6 Correlation of the SFXN family gene expression with the AR score (**A**–**C**) or NEPC score (**D**–**E**) in CRPC patients. Gene expression at the mRNA levels (log_2 [TPM + 1]) was extracted from the SU2C/PCF dataset on the cBioportal platform. The asterisk indicates a significant difference between the two groups

Discussion

In this study, our analysis determined that SFXN1/3/4 genes were predominantly expressed in prostate tissue, of which SFXN1/4 were mainly expressed in luminal cells while the SFXN3 gene was expressed in basal cells at a relatively higher level. In primary prostate cancers, SFXN2/SFXN4 expressions were significantly upregulated but SFXN3 expression was downregulated compared to benign tissues. SFXN4 expression exerted as a strong diagnostic factor for prostate cancer and a prognostic factor for patient survival outcomes. Although there were no molecular signature-specific dysregulations of the SFXN family genes, SFXN3 expression was broadly correlated with most pro-inflammatory immune infiltrations while SFXN4 expression was strongly correlated with three proinflammatory lymphocytes (Th1 cells, Neutrophils, and NK cells). In CRPC tumors, SFXN2/SFXN4 expressions were positively correlated with AR scores while negatively correlated with NEPC scores. Consistently, SFXN2/SFXN4 expressions were decreased in prostate cells after castration in animal models.

Upregulation of SFXN2/SFXN4 expression has been observed in human cancers, where their expression levels associated with diverse prognostic outcomes depending on the type of cancer [6, 34, 39, 40]. SFXN2 expression was particularly significant in breast cancer, where it was upregulated and linked to cancer cell growth [39]. This association makes it a potential biomarker for breast cancer prognosis and a possible target for therapeutic intervention. SFXN4 is gaining attention as a prognostic marker due to its role in oxidative phosphorylation and its correlation with immune infiltration in tumors. For example, higher SFXN4 expression in hepatocellular carcinoma (HCC) correlates with increased tumor aggressiveness and specific immune profiles, suggesting SFXN4 could be a therapeutic target for mitochondrial-based cancer treatments [40]. In our study, we also found SFXN2/SFXN4 overexpression in prostate cancers, of which only SFXN4 expression was tightly associated with immune infiltration and disease progression. Particularly, we determined for the first time that SFXN2/SFXN4 expressions were strongly associated with the AR signaling scores and were decreased in castrated animals.

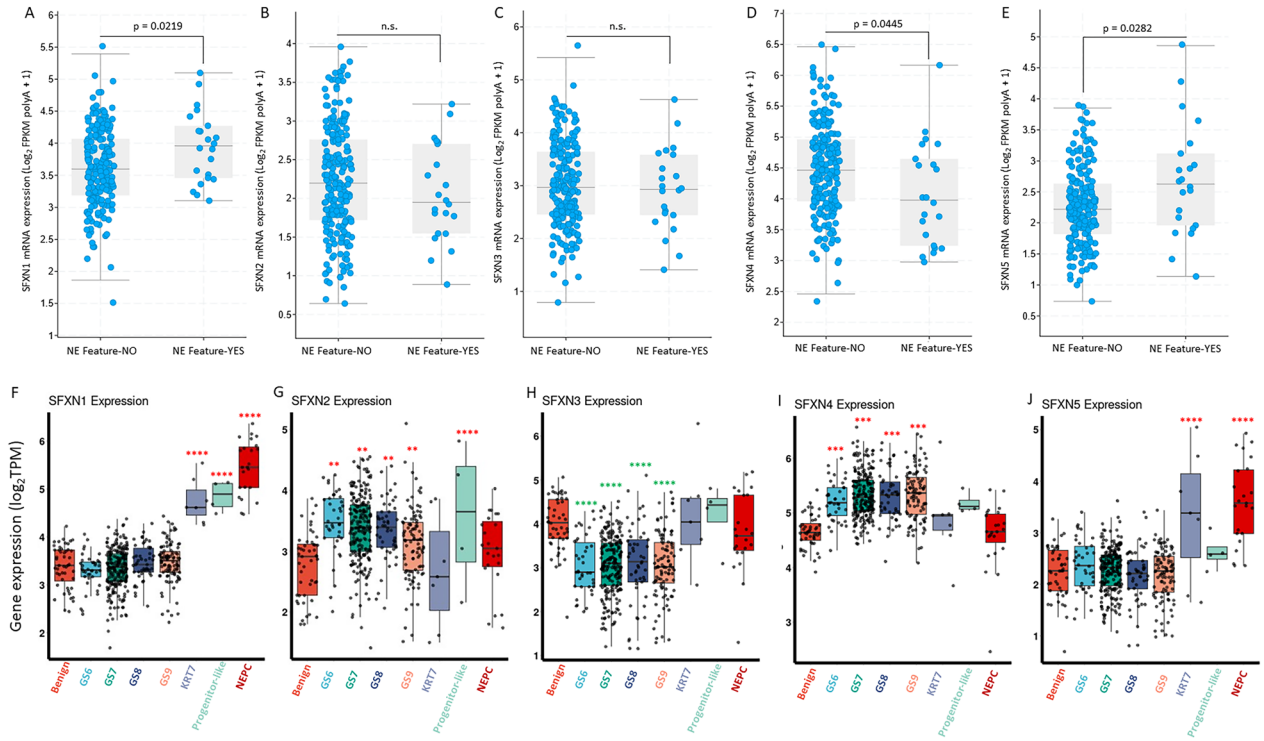

Fig. 7 Expression of the SFXN family genes in CRPC patients. **A**–**E** CRPC tissues without NE or with NE features were divided into two groups for comparison of SFXN expressions. Data at the mRNA levels were shown as $\log_2$[FPKM + 1] values extracted from the SU2C/PCF dataset on the cBioportal platform. The p-values shown in each panel were derived from Student's t-test. **F**–**J** The mRNA expression levels of SFXN family genes were compared in subgroups based on tumor pathological features, as indicated. The asterisks indicate a significant difference from ANOVA analysis. Red asterisks, upregulation vs the benign control; green asterisks, downregulation vs the benign control. **** $p < 0.001$, ** $p < 0.01$

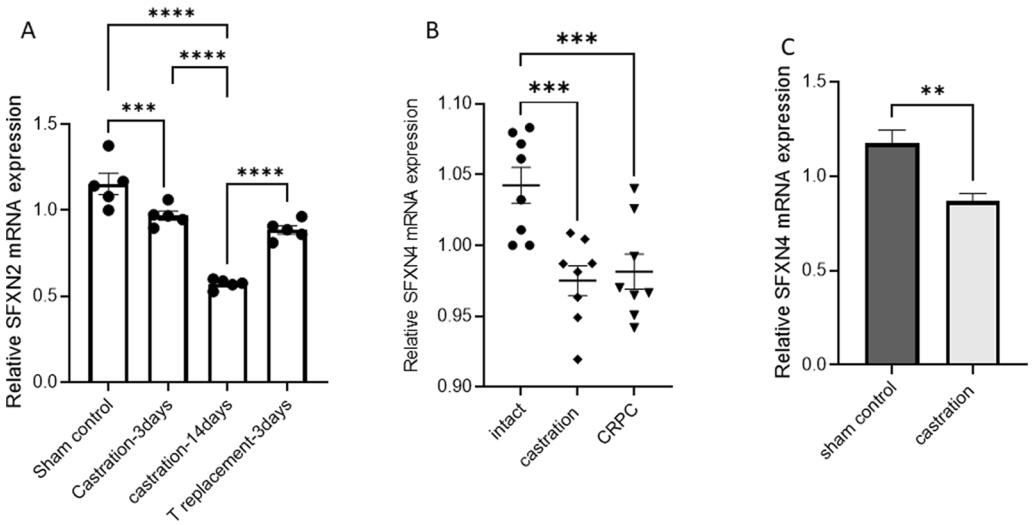

Fig. 8 Expression of SFXN2/4 genes in mouse prostate or human prostate xenografts in nude mice after castration or testosterone replacement. Microarray data were extracted from the NCBI GEO profiles of GDS2562 (**A**), GDS4107 (**B**), and GDS4120 (**C**). The relative values were calculated against the lowest value in the control group before statistical analysis. The asterisk indicates a significant difference. Student's *t*-test, ** $p < 0.01$; **** $p < 0.0001$

Further investigation is needed to understand their functional roles in CRPC progression.

SFXN3 has revealed its role in different types of cancer, making it a protein of interest for therapeutic targeting [39, 41–45]. In head and neck squamous cell carcinoma (HNSC), SFXN3 expression was correlated with poor prognosis, chemotherapy resistance, and an immune suppressive tumor microenvironment [43]. This regulation is thought to involve a non-coding RNA pathway (LINC01270/hsa-miR-29c-3p/SFXN3), suggesting that SFXN3 might contribute to aggressive tumor behaviors by modulating immune responses and drug resistance mechanisms. In this study, we observed a broad and strong correlation of SFXN3 expression with pro-inflammatory immune infiltration in prostate cancers. Since SFXN3 expression was reduced in prostate cancer, suggesting an enhanced expression of the SFXN3 gene might be able to sensitize prostate cancer to immunotherapy. In hematological cancers, such as non-M3 acute myeloid leukemia (AML), high SFXN3 levels have been associated with unfavorable outcomes. Here, SFXN3 may increase sensitivity to hypomethylating therapies, like decitabine, offering potential treatment avenues in cases where other therapies have been ineffective. This finding opens new possibilities for using SFXN3 as a biomarker in treatment strategies tailored to AML patients with high SFXN3 expression [45].

SFXN1 has been identified as a potential biomarker in multiple human cancers [39, 46–48], including lung adenocarcinoma [46, 49–53]. Its high expression was correlated with factors like tumor size and metastasis, and it is associated with immune infiltration. In human lung cancers, SFXN1 expression influenced the tumor microenvironment by interacting with immune cells, such as T and B cells, and immune checkpoints [53]. This suggests that SFXN1 could be targeted for immune-based therapies in cancers like lung cancer. In our study, SFXN1 expression was strongly correlated with a few pro-inflammatory immune infiltrations, although its expression levels were not significantly altered in malignant tissues.

Recent research into SFXN5 has uncovered its role in neutrophil function and immune response, primarily through regulating actin polymerization [7]. SFXN5, identified as a citrate transporter in vitro, is critical for neutrophil spreading, an initial step in adhesion and migration essential for immune response [7]. SFXN5 deficiency in neutrophils (induced via siRNA or morpholino injection in mice and zebrafish models) led to impaired cell spreading, adhesion, chemotaxis, and reactive oxygen species production. This deficiency also reduced actin polymerization due to lower cytosolic citrate levels and downstream metabolites like acetyl-CoA and cholesterol, which are necessary for actin polymerization mediated by phosphatidylinositol 4,5-bisphosphate (PI (4,5) P2). Supplementing with citrate or cholesterol partially restored these processes, highlighting SFXN5's pivotal role in cellular actin dynamics and neutrophil migration during inflammatory responses. In this study, we found that SFXN5 was expressed at a very low level in prostate tissue, both benign and malignant. SFXN5 expression was not associated with disease progression and immune infiltration. However, SFXN5 expression was highly expressed in NEPC cells, both cell line and patient tissues, especially the newly identified KRT7 subtype. These data suggest that SFXN5's role in prostate cancer is focused on KRT7-related NEPC progression.

In conclusion, our profiling analysis of SFXN family genes in prostate cancers revealed a diverse profile, of which SFXN2/SFXN4 genes were upregulated while SFXN3 was downregulated. SFXN2/SFXN4 expression was associated with prostate cancer progression and was positively modulated by the AR signal pathway. Most importantly, SFXN4 expression exerted as a strong biomarker for disease diagnosis and overall survival outcome.

Acknowledgements
The results shown in this study are in part based on data generated by the TCGA Research Network (https://www.cancer.gov/tcga) and the HuPSA Single-cell Sequencing data platform (https://pcatools.shinyapps.io/HuPSA-MoPSA/).

Author contributions
H Huang, H Lian, and B Li conducted the data analysis. W Liu conducted the real-time qPCR experiments and data analysis. H Shao, R Zhu, and B Li drafted the manuscript. All authors approved the submission.

Funding
This work was partially supported by the Hangzhou Zijingang Science & Technology City High-level Talent Plan Category B to Dr. Runzhi Zhu.

Availability of data and materials
Not applicable

Declarations

Ethics approval and consent to participate
Not applicable.

Competing interests
The authors declared no commercial or financial relationships construed as a potential conflict of interest.

Received: 12 November 2024 Accepted: 11 December 2024
Published online: 07 February 2025

References

1. Tifoun N, De Las Heras JM, Guillaume A, Bouleau S, Mignotte B, Le Floch N. Insights into the roles of the sideroflexins/SLC56 family in iron homeostasis and iron-sulfur biogenesis. Biomedicines. 2021;9(2):103.

2. Attwood MM, Schioth HB. Characterization of five transmembrane proteins: with focus on the tweety, sideroflexin, and YIP1 domain families. Front Cell Dev Biol. 2021;9:708754.
3. Kory N, Wyant GA, Prakash G, Uit de Bos J, Bottanelli F, Pacold ME, Chan SH, Lewis CA, Wang T, Keys HR, et al. SFXN1 is a mitochondrial serine transporter required for one-carbon metabolism. Science. 2018;362:6416.
4. Paul BT, Tesfay L, Winkler CR, Torti FM, Torti SV. Sideroflexin 4 affects Fe-S cluster biogenesis, iron metabolism, mitochondrial respiration and heme biosynthetic enzymes. Sci Rep. 2019;9(1):19634.
5. Jackson TD, Crameri JJ, Muellner-Wong L, Frazier AE, Palmer CS, Formosa LE, Hock DH, Fujihara KM, Stait T, Sharpe AJ, et al. Sideroflexin 4 is a complex I assembly factor that interacts with the MCIA complex and is required for the assembly of the ND2 module. Proc Natl Acad Sci USA. 2022;119(13):e2115566119.
6. Tesfay L, Paul BT, Hegde P, Brewer M, Habbani S, Jellison E, Moore T, Wu H, Torti SV, Torti FM. Complementary anti-cancer pathways triggered by inhibition of sideroflexin 4 in ovarian cancer. Sci Rep. 2022;12(1):19936.
7. Zhang H, Meng L, Liu Y, Jiang J, He Z, Qin J, Wang C, Yang M, He K, Yang J, et al. Sfxn5 regulation of actin polymerization for neutrophil spreading depends on a citrate-cholesterol-PI(4,5)P2 pathway. J Immunol. 2023;211(3):462–73.
8. Rafikova G, Gilyazova I, Enikeeva K, Pavlov V, Kzhyshkowska J. Prostate cancer: genetics, epigenetics and the need for immunological biomarkers. Int J Mol Sci. 2023;24(16):12797.
9. Boehm BE, York ME, Petrovics G, Kohaar I, Chesnut GT. Biomarkers of aggressive prostate cancer at diagnosis. Int J Mol Sci. 2023;24(3):2185.
10. Uhr A, Glick L, Gomella LG. An overview of biomarkers in the diagnosis and management of prostate cancer. Can J Urol. 2020;27(S3):24–7.
11 Kohaar I, Petrovics G, Srivastava S. A rich array of prostate cancer molecular biomarkers: opportunities and challenges. Int J Mol Sci. 2019;20(8):1813.
12. Oudes AJ, Campbell DS, Sorensen CM, Walashek LS, True LD, Liu AY. Transcriptomes of human prostate cells. BMC Genom. 2006;7:92.
13. Ghandi M, Huang FW, Jane-Valbuena J, Kryukov GV, Lo CC, McDonald ER 3rd, Barretina J, Gelfand ET, Bielski CM, Li H, et al. Next-generation characterization of the cancer cell line encyclopedia. Nature. 2019;569(7757):503–8.
14. Xu H, Liu W, He C, Mirza M, Li B. Aberrant expression of multiple glycolytic enzyme genes is significantly associated with disease progression and survival outcomes in prostate cancers. Am J Clin Exp Urol. 2023;11(6):530–41.
15. Huang H, Song S, Liu W, Ye S, Bao Y, Mirza M, Li B, Huang J, Zhu R, Lian H. Expressions of glucose transporter genes are diversely attenuated and significantly associated with prostate cancer progression. Am J Clin Exp Urol. 2023;11(6):578–93.
16. He C, Liu W, Sun J, Zhang D, Li B. Jumonji domain-containing protein RIOX2 is overexpressed and associated with worse survival outcomes in prostate cancers. Front Oncol. 2023;13:1087082.
17. Huang J, Liu W, Zhang D, Lin B, Li B. TMEM158 expression is negatively regulated by AR signaling and associated with favorite survival outcomes in prostate cancers. Front Oncol. 2022;12:1023455.
18. Huang J, Liu W, Lin BY, Li JC, Lu J, Li BY. Scaffold protein MAPK8IP2 expression is a robust prognostic factor in prostate cancer associated with AR signaling activity. Asian J Androl. 2023;25(2):198–207.
19. Tao C, Liu W, Yan X, Yang M, Yao S, Shu Q, Li B, Zhu R. PAQR5 expression is suppressed by TGFbeta1 and associated with a poor survival outcome in renal clear cell carcinoma. Front Oncol. 2021;11:827344.
20. Yang M, Li JC, Tao C, Wu S, Liu B, Shu Q, Li B, Zhu R. PAQR6 upregulation is associated with AR signaling and unfavorite prognosis in prostate cancers. Biomolecules. 2021;11(9):1383.
21. Huang J, Liu W, Song S, Li JC, Gan K, Shen C, Holzbeierlein J, Li B. The iron-modulating hormone hepcidin is upregulated and associated with poor survival outcomes in renal clear cell carcinoma. Front Pharmacol. 2022;13:1080055.
22. Wang J, Liu W, Li JC, Li M, Li B, Zhu R. Hepcidin downregulation correlates with disease aggressiveness and immune infiltration in liver cancers. Front Oncol. 2021;11:714756.
23. Menyhart O, Nagy A, Gyorffy B. Determining consistent prognostic biomarkers of overall survival and vascular invasion in hepatocellular carcinoma. R Soc Open Sci. 2018;5(12):181006.
24. Abida W, Cyrta J, Heller G, Prandi D, Armenia J, Coleman I, Cieslik M, Benelli M, Robinson D, Van Allen EM, et al. Genomic correlates of clinical outcome in advanced prostate cancer. Proc Natl Acad Sci USA. 2019;116(23):11428–36.
25. Cheng S, Li L, Yeh Y, Shi Y, Franco O, Corey E, Yu X. Unveiling novel double-negative prostate cancer subtypes through single-cell RNA sequencing analysis. NPJ Precis Oncol. 2024;8(1):171.
26. Wang XD, Wang BE, Soriano R, Zha J, Zhang Z, Modrusan Z, Cunha GR, Gao WQ. Expression profiling of the mouse prostate after castration and hormone replacement: implication of H-cadherin in prostate tumorigenesis. Differentiation. 2007;75(3):219–34.
27. Sun Y, Wang BE, Leong KG, Yue P, Li L, Jhunjhunwala S, Chen D, Seo K, Modrusan Z, Gao WQ, et al. Androgen deprivation causes epithelial-mesenchymal transition in the prostate: implications for androgen-deprivation therapy. Cancer Res. 2012;72(2):527–36.
28. Terada N, Shimizu Y, Kamba T, Inoue T, Maeno A, Kobayashi T, Nakamura E, Kamoto T, Kanaji T, Maruyama T, et al. Identification of EP4 as a potential target for the treatment of castration-resistant prostate cancer using a novel xenograft model. Cancer Res. 2010;70(4):1606–15.
29. Pacini C, Dempster JM, Boyle I, Goncalves E, Najgebauer H, Karakoc E, van der Meer D, Barthorpe A, Lightfoot H, Jaaks P, et al. Integrated cross-study datasets of genetic dependencies in cancer. Nat Commun. 2021;12(1):1661.
30. Dempster JM, Boyle I, Vazquez F, Root DE, Boehm JS, Hahn WC, Tsherniak A, McFarland JM. Chronos: a cell population dynamics model of CRISPR experiments that improves inference of gene fitness effects. Genome Biol. 2021;22(1):343.
31. Liu W, He C, Li C, Ye S, Zhao J, Zhu C, Wang X, Ma Q, Li B. Natural compound alternol actives multiple endoplasmic reticulum stress-responding pathways contributing to cell death. Front Pharmacol. 2024;15:1397116.
32. Tang Y, Chen R, Huang Y, Li G, Huang Y, Chen J, Duan L, Zhu BT, Thrasher JB, Zhang X, et al. Natural compound alternol induces oxidative stress-dependent apoptotic cell death preferentially in prostate cancer cells. Mol Cancer Ther. 2014;13(6):1526–36.
33. Liao X, Tang S, Thrasher JB, Griebling TL, Li B. Small-interfering RNA-induced androgen receptor silencing leads to apoptotic cell death in prostate cancer. Mol Cancer Ther. 2005;4(4):505–15.
34. Chen Y, Qian J, Ding P, Wang W, Li X, Tang X, Tang C, Yang Y, Gu C. Elevated SFXN2 limits mitochondrial autophagy and increases iron-mediated energy production to promote multiple myeloma cell proliferation. Cell Death Dis. 2022;13(9):822.
35. Mon EE, Wei FY, Ahmad RNR, Yamamoto T, Moroishi T, Tomizawa K. Regulation of mitochondrial iron homeostasis by sideroflexin 2. J Physiol Sci. 2019;69(2):359–73.
36. Cancer Genome Atlas Research N. The molecular taxonomy of primary prostate cancer. Cell. 2015;163(4):1011–25.
37. Gao D, Shen Y, Xu L, Sun Y, Hu H, Xu B, Wang Z, Xu H. Acetate utilization promotes hormone therapy resistance in prostate cancer through neuroendocrine differentiation. Drug Resist Updat. 2024;77:101158.
38. Ge R, Wang Z, Montironi R, Jiang Z, Cheng M, Santoni M, Huang K, Massari F, Lu X, Cimadamore A, et al. Epigenetic modulations and lineage plasticity in advanced prostate cancer. Ann Oncol. 2020;31(4):470–9.
39. Yuan D, Liu J, Sang W, Li Q. Comprehensive analysis of the role of SFXN family in breast cancer. Open Med (Wars). 2023;18(1):20230685.
40. Du Z, Zhang Z, Han X, Xie H, Yan W, Tian D, Liu M, Rao C. Comprehensive analysis of sideroflexin 4 in hepatocellular carcinoma by bioinformatics and experiments. Int J Med Sci. 2023;20(10):1300–15.
41. Dong Y, Jin F, Wang J, Li Q, Huang Z, Xia L, Yang M. SFXN3 is associated with poor clinical outcomes and sensitivity to the hypomethylating therapy in non-M3 acute myeloid leukemia patients. Curr Gene Ther. 2023;23(5):410–8.
42. Jin F, He L, Wang J, Zhang Y, Yang M. SFXN3 is a prognostic marker and promotes the growth of acute myeloid leukemia. Cell Biochem Biophys. 2024;82(3):2195–204.
43. Chen K, Gong S, Fang X, Li Q, Ye M, Li J, Huang S, Zhao Y, Liu N, Li Y, et al. Non-coding RNA-mediated high expression of SFXN3 as a prognostic biomarker associated with paclitaxel resistance and immunosuppressive microenvironment in head and neck cancer. Front Immunol. 2022;13:920136.

44. Jin T, Ge L, Chen J, Wang W, Zhang L, Ge M. Identification of iron metabolism-related genes as prognostic indicators for papillary thyroid carcinoma: a retrospective study. PeerJ. 2023;11:e15592.
45. Zhou H, Wang F, Niu T. Prediction of prognosis and immunotherapy response of amino acid metabolism genes in acute myeloid leukemia. Front Nutr. 2022;9:1056648.
46. Li Y, Yang W, Liu C, Zhou S, Liu X, Zhang T, Wu L, Li X, Zhang J, Chang E. SFXN1-mediated immune cell infiltration and tumorigenesis in lung adenocarcinoma: a potential therapeutic target. Int Immunopharmacol. 2024;132:111918.
47. Andriani L, Ling YX, Yang SY, Zhao Q, Ma XY, Huang MY, Zhang YL, Zhang FL, Li DQ, Shao ZM. Sideroflexin-1 promotes progression and sensitivity to lapatinib in triple-negative breast cancer by inhibiting TOLLIP-mediated autophagic degradation of CIP2A. Cancer Lett. 2024;597:217008.
48. Yagi K, Shimada S, Akiyama Y, Hatano M, Asano D, Ishikawa Y, Ueda H, Watanabe S, Akahoshi K, Ono H, et al. Loss of SFXN1 mitigates lipotoxicity and predicts poor outcome in non-viral hepatocellular carcinoma. Sci Rep. 2023;13(1):9449.
49. Zhang YH, Liu XS, Gao Y, Yuan LL, Huang ZM, Zhang Y, Liu ZY, Yang Y, Liu XY, Ke CB, et al. SFXN1 as a potential diagnostic and prognostic biomarker of LUAD is associated with (18)F-FDG metabolic parameters. Lung Cancer. 2024;188:107449.
50. Liu W, Du Q, Mei T, Wang J, Huang D, Qin T. Comprehensive analysis the prognostic and immune characteristics of mitochondrial transport-related gene SFXN1 in lung adenocarcinoma. BMC Cancer. 2024;24(1):94.
51. Chen L, Kang Y, Jiang Y, You J, Huang C, Xu X, Chen F. Overexpression of SFXN1 indicates poor prognosis and promotes tumor progression in lung adenocarcinoma. Pathol Res Pract. 2022;237:154031.
52. Chen Q, Wang R, Zhang J, Zhou L. Sideroflexin1 as a novel tumor marker independently predicts survival in lung adenocarcinoma. Transl Cancer Res. 2019;8(4):1170–8.
53. Dang HH, Ta HDK, Nguyen TTT, Anuraga G, Wang CY, Lee KH, Le NQK. Prospective role and immunotherapeutic targets of sideroflexin protein family in lung adenocarcinoma: evidence from bioinformatics validation. Funct Integr Genom. 2022;22(5):1057–72.

Publisher's Note